



AAS/AIAA Astrodynamics Conference

Reducing Conservatism of Analytic Transient Response Bounds via Shaping Filters

**Aiyueh Kwan, Nazareth Bedrossian, Jiann-Woei Jang
The Charles Stark Draper Laboratory, Inc.**

and

**Karolos Grigoriadis
University of Houston**

**Westin Prince Alyeska Resort
Girdwood, Alaska**

August 16-19, 1999

General Chairs

AAS

**Bernard Kaufman
Naval Research Laboratory**

AIAA

**Kyle Alfriend
Texas A&M University**

Technical Chairs

**Kathleen Howell
Purdue University**

**Felix Hoots
GRC International, Inc.**

Reducing Conservatism of Analytic Transient Response Bounds via Shaping Filters

Aiyueh Kwan¹, Nazareth Bedrossian², Jiann-Woei Jang³
The Charles Stark Draper Laboratory, Inc.,
2200 Space Park Dr, Suite 210
Houston, TX 77058

Karolos Grigoriadis⁴
Department of Mechanical Engineering
University of Houston
Houston, TX 77204

Abstract

Recent results show that the peak transient response of a linear system to bounded energy inputs can be computed using the energy-to-peak gain of the system. However, analytically computed peak response bound can be conservative for a class of bounded energy signals, specifically pulse trains generated from jet firings encountered in space vehicles. In this paper, shaping filters are proposed as a methodology to reduce the conservatism of peak response analytic bounds. This methodology was applied to a realistic Space Station assembly operation subject to jet firings. The results indicate that shaping filters indeed reduce the predicted peak response bounds.

1. Introduction

Assembly of the International Space Station requires robotic manipulation of various payloads. The payloads will be manipulated by the Shuttle Remote Manipulator System (SRMS), the Space Station Remote Manipulator System (SSRMS). During assembly operations, it may be necessary to execute corrective attitude control thruster firings. The operational plan requires stopping the robotic payload operation and activating the SRMS/SSRMS joint brakes before firing attitude control thrusters. Hence, to evaluate the feasibility of planned robotic operations, it is necessary to show that the joint brakes do not slip during thruster firings.

¹ Graduate Student, Department of Mechanical Engineering, University of Houston

² Senior Member Technical Staff, The Charles Stark Draper Laboratory

³ Member Technical Staff II, The Charles Stark Draper Laboratory

⁴ Associate Professor, Department of Mechanical Engineering, University of Houston

To evaluate the feasibility of thruster firings when the robotic systems are in the brakes-on mode requires evaluating the maximum joint torque and comparing that with a brake slip limit torque. Typical attitude control firings include bipolar pulse trains representing attitude maneuvers and unipolar pulse trains for attitude hold or momentum desaturation. The standard approach to evaluate the peak brakes-on joint torque is via time-domain simulations. This approach can be time consuming and inefficient since time-domain simulations can only calculate the peak response to one pulse train at a time. Thus, it is difficult to map the time-domain simulation results to a family or class of pulse trains.

Recent results [1,2] in linear operator norm theory show that the peak transient response of a linear system to bounded energy inputs can be computed using the energy-to-peak gain of the system. This computation requires the solution of a Lyapunov equation of order equal to the order of the system. The energy-to-peak gain theory also provides the worst-case input that will result in the transient response reaching its peak. It is noted that the bounds provided by this theory are tight, that is, the bounds are achievable by a certain input excitation.

The class of all energy-bounded input signals considered in the energy-to-peak gain theory is a very broad one for practical applications. Hence, the analytically computed peak response bounds can be conservative for practical classes of bounded energy signals, such as, pulse trains generated from jet firings encountered in space vehicles. In this paper, shaping filters are proposed as a methodology to reduce the conservatism of peak response analytic bounds computed by the energy-to-peak gain theory. A filter design procedure corresponding to a given class of input signals is presented for conservatism reduction, and the methodology is illustrated using two types of input signals for a realistic example involving Space Station robotic assembly.

The notation to be used in this paper is as follows: $\|u\|_{L_2}$ denotes the energy (or 2-norm) of a signal u , that is,

$$\|u\|_{L_2} = \left(\int_0^{\infty} u(t)^T u(t) dt \right)^{1/2}$$

and $\|u\|_{L_\infty}$ denotes the peak (or infinity) norm of a signal u , that is

$$\|u\|_{L_\infty} = \max_i |u_i(t)|.$$

For a matrix A , $\|A\|$ denotes the maximum singular value (or induced 2-norm) of the matrix.

2. Worst-Case Energy-to-Peak Gain

We consider the energy-to-peak gain response of linear time-invariant (LTI) systems. The specific application of interest is the computation of peak response bounds for robotic assembly of the International Space Station (ISS) subject to thruster firings. Mathematical modeling of the ISS robotic assembly results in high-order nonlinear models that contain linear structural dynamic effects and nonlinear robot arm dynamic effects. Since the operational scenario under consideration is static and the response of the robotic system is dominated by its local behavior, a linear representation is appropriate if the non-linear brakes-on behavior is

approximated by a linear equivalent. This can be accomplished by modeling the brakes-on dynamics by an equivalent linear stiffness. With this assumption, a linear time-invariant model from thruster inputs to joint torques can be obtained. Then, consider a linear time-invariant system, $G(s)$, which has the state space form as follows,

$$\begin{aligned}\dot{x} &= Ax + Bu \\ y &= Cx\end{aligned}$$

where u is the input pulse train. The objective is to estimate the peak pulse response of the above system without a time-domain simulation. This can be accomplished by making use of the energy-to-peak gain of the system.

The peak transient response of a linear time-invariant system to bounded energy input signals can be computed from the energy-to-peak gain (L_2 -to- L_∞ gain) of the relevant transfer function [1]:

$$\Gamma_{ep} \equiv \sup_{\|u\|_{L_2} \leq 1} \|y\|_{L_\infty} \quad (1)$$

Hence, the energy-to-peak gain provides the worst-case peak response for the class of all unit-energy bounded signals. This gain can be computed from the following result [1,2]

$$\Gamma_{ep} = \|CXC^T\|^{1/2}$$

where X is the controllability grammian of the system, which must satisfy the linear Lyapunov equation:

$$AX + XA^T + BB^T = 0$$

Hence, the energy-to-peak gain can be computed by solving a Lyapunov equation of order equal to the order n of the system. Efficient Bartels-Stewart algorithms can solve the Lyapunov equation requiring $O(n^2)$ floating point operations [3]. The symmetric solution can also be solved by use of the Kronecter product [4]. For very large-scale systems approximate solutions can be computed very efficiently using Krylov-subspace methods [5].

The above standard formulation of the energy-to-peak gain theory provides a tight upper bound as well as a method to construct the particular input signal for which the bound is reached. Hence, a straightforward application of this approach to a specific class of inputs, such as, thruster pulse trains can be very conservative. The conservatism is due to the fact that the standard formulation cannot, for example, distinguish between unit-norm bipolar and unit-norm unipolar pulses since both pulse trains have unit norm, resulting in the same estimate for the peak response. On the other hand, these signals generate very different time-domain signatures resulting in different peak responses. Thus, direct application of this method to practical problems involving specific classes of inputs would result in conservative estimates due the large class of input signals it allows.

One approach to improve the peak response estimate is to restrict the allowable class of signals by preshaping the input signal so that it corresponds to a desired class of practical signals. From (1) it is apparent that the input signal u can be preshaped by a linear operator F resulting in a new input signal w , such that, $u = Fw$, as long as its induced 2-norm is less than one. In this case, the fictitious input w is any unit-energy bounded signal and F is selected so that Fw approximates the desired class of input signals. Hence, F can be used to shape or optimize the

resulting peak estimate. In this paper, a method to design such shaping filters is proposed to reduce the conservatism of the energy-to-peak gain for pulse train input signals. However, the methods can be generalized to any specified class of input signals.

3. Shaping Filter Design

The fundamental shaping filter design strategy is to exploit the frequency domain characterization of thruster pulse trains, specifically its power spectral density function, in order to design shaping filters that match the signal frequency content. The frequency domain representation of the input signals provides the ability to discriminate between similar norm signals. For the example presented in the previous section, the power spectral density (PSD) representation of unit norm bipolar and unipolar signals clearly allows for discrimination among these inputs. From the power spectrum of the input signal, filters can be designed such that the power spectrum of the filtered signal matches that of the input signal.

Given a characteristic input or class of inputs in the time domain the corresponding filters can be designed by solving a frequency-based interpolation problem. First the Fast Fourier transform(s) (FFTs) of the input signals is calculated, and then a continuous-time filter, which corresponds to the FFT of the pulse train, is computed using any one of many standard interpolation algorithms. In our case we use the MATLAB function *invfreqs* to solve for the filter interpolation [6]. Assume the filter transfer function has the following form:

$$F(s) = \frac{B(s)}{A(s)} = \frac{b_n s^n + b_{n-1} s^{n-1} + \dots + b_1 s^1 + b_0}{a_n s^n + a_{n-1} s^{n-1} + \dots + a_1 s^1 + a_0}$$

The coefficients of the numerator and denominator are determined by the minimal of the following cost function [6],

$$\min_{a,b} \sum_{k=1}^n wt(k) |F(k)A(k) - B(k)|^2$$

where $wt(k)$ is a user specified weighting function. In our approach, only peak PSD response frequencies were selected and used in the solution of filter coefficients to avoid solving a large system equation. The magnitude at each peak response was selected to be the weighting function, $wt(k)$.

To guarantee existence of the Lyapunov solution [7], the filter has to be stable since the original system is stable. This can be implemented by removing the unstable poles of the filter. Once the filter has been formed, it is then normalized in order to achieve an induced 2-norm equal to 1. The filter is then concatenated with the original system resulting in the augmented plant:

$$\overline{G}(s) = G(s)F(s)$$

where $G(s)$ is the transfer function of the LTI plant and $F(s)$ is the transfer function of the shaping filter. The augmented plant is then used to compute the energy-to-peak gain.

4. Test Case Results

In this paper, the International Space Station assembly stage 4A is used to illustrate the improvement in peak response estimate using the energy-to-peak gain formulation and shaping filters. The testcase represents the US Lab installation using the SRMS shown in Figure 1. The testcase corresponds to the US Lab in the Pitch 180 configuration with the SRMS in brakes-on mode. The output variables of interest are the SRMS joint torques, shoulder yaw (SHY), shoulder pitch (SHP), elbow pitch (ELP), wrist pitch (WRP), wrist yaw (WRY), and wrist roll (WRR). The input signals are typical bipolar and unipolar thruster pulsetrains. The 2-pulse bipolar pulsetrain is shown in Figure 1 and consists of 20sec thruster firing time, 75sec delay between thruster firing, and the signal is sampled at 0.2sec. The PSD of the pulse train and the shaping filter are shown in Figure 3. The frequency response of the shaping filter is shown in Figure 5. The 5-pulse unipolar pulsetrain is shown in Figure 5 and consists of 1sec thruster firing time, delays of 17.8, 11.4, 8.8, and 14sec between thruster firing, and the signal is sampled at 0.2sec. The PSD of the pulse train and the shaping filter are shown in Figure 6. The frequency response of the shaping filter is shown in Figure 7.

The SRMS joint torque peak response is computed from simulation and compared to the estimates produced by the standard formulation (unweighted) and shaping filter formulation (weighted) of the energy-to-peak gain. The peak response is obtained for three pure single axis (roll, pitch, yaw) and a single multiaxis thruster pulsetrain testcases. The results for the bipolar inputs are shown in Table 1, while those for the unipolar input are given in Table 2. For the bipolar input testcase, Table 1, it is evident that the unweighted results substantially overestimate the peak response when compared to the simulation results. The overestimate is on average approximately 760% of the simulation peak response. The weighted results on the other hand reduce the overestimate by approximately 75%. For the unipolar testcase, Table 2, it is evident that the unweighted results also substantially overestimate the peak response when compared to the simulation results. The overestimate is on average approximately 860% of the simulation peak response. The weighted results reduce the overestimate by approximately 50%. Further, the overestimate in the weighted results can be attributed to errors in interpolating the frequency content of the input signal.

5. Conclusion

In this paper, shaping filters were proposed as a means to reduce the conservatism of analytical peak response estimates due to thruster pulse trains using the energy-to-peak gain formulation. The methodology was illustrated using two types of input signals for a realistic example involving Space Station robotic assembly. The results indicated that the use of shaping filters indeed does reduce the analytic peak response bounds substantially. Improved filter interpolation algorithms are expected to result in further improvements in the analytic estimates.

6. References

1. Skelton, R., Iwasaki, T., and Grigoriadis, K., *A Unified Algebraic Approach to Linear Control Design*, Taylor & Francis, 1998.
2. Peterson, L. D., "Bounding the Transient Response of Structures to Uncertain Disturbances," *AIAA Journal*, Vol. 34, No. 6, June 1996, pp. 1245-1249.
3. Bartels, R.H., and Stewart, G.W., "Solution of the Matrix Equation $AX+XB=C$," *Communications of the Association for Computer Machinery*, Vol. 15, No. 2, 1972, pp. 820-826.
4. Jang, J.-W., and Fitz-Coy, N. G., "An Efficient and Robust Homotopy algorithm for the Algebraic Riccati Equation," SIAM annual meeting, Charlotte, N. C., Oct. 23-26, 1995.
5. Sidi-Ali-Cherif, S., Grigoriadis, K.M., and Subramaniam, M., "Model Reduction of Large Space Structures Using Approximate Component Cost Analysis," *AIAA Journal of Guidance, Control, and Dynamics*, Vol. 22, No. 4, 1999, pp. 551-557.
6. Levi, E. C., "Complex-Curve Fitting," *IRE Transaction on Automatic Control*, vol. AC-4, 1959, pp. 37-44.
7. Graham, A., *Kronecker Products and Matrix Calculus: with Application*, Ellis Horwood Limited, 1981.

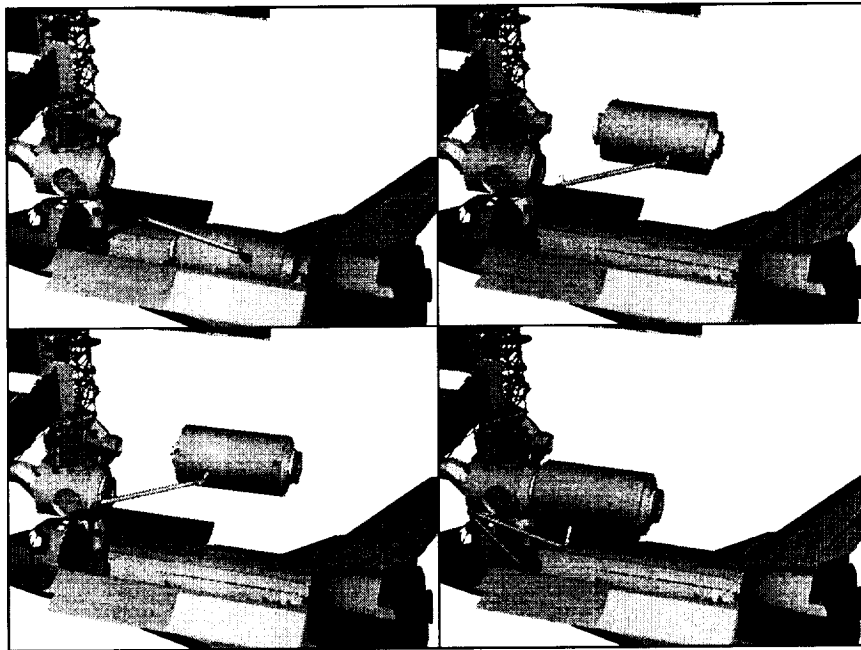


Figure 1. Stage 4A SRMS US Lab installation intermediate configurations

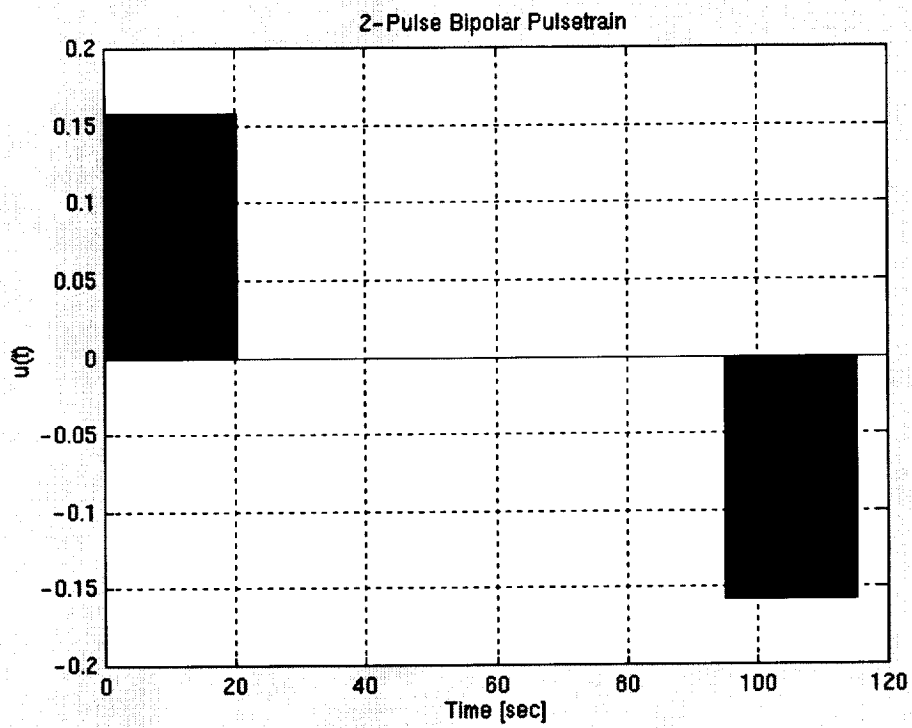


Figure 2. 2-pulse Bipolar Signal

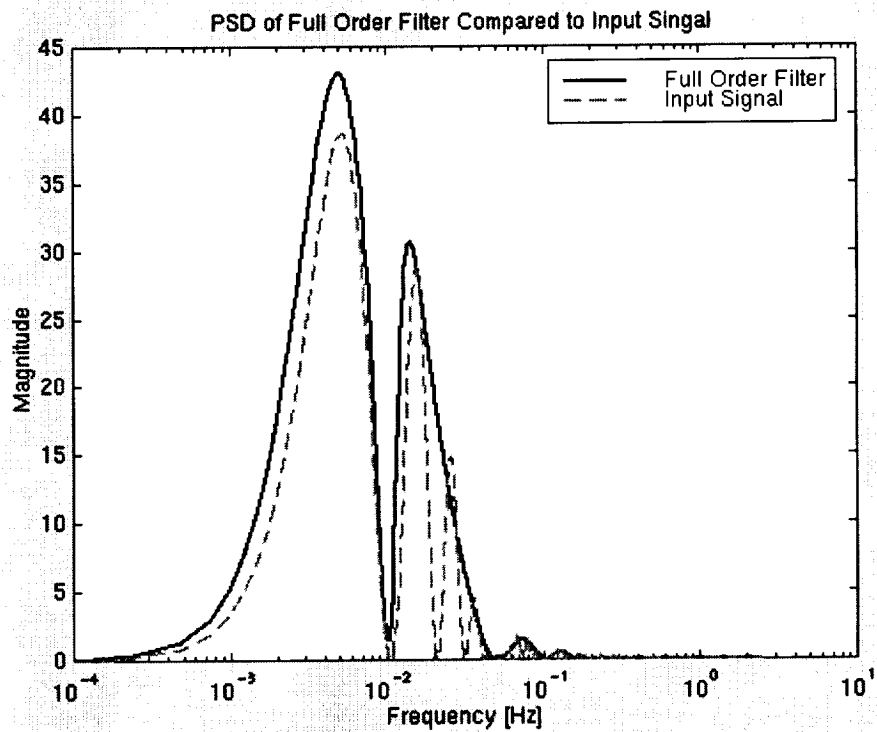


Figure 3. PSD of Filtered Signal Compared to 2-pulse Bipolar Signal

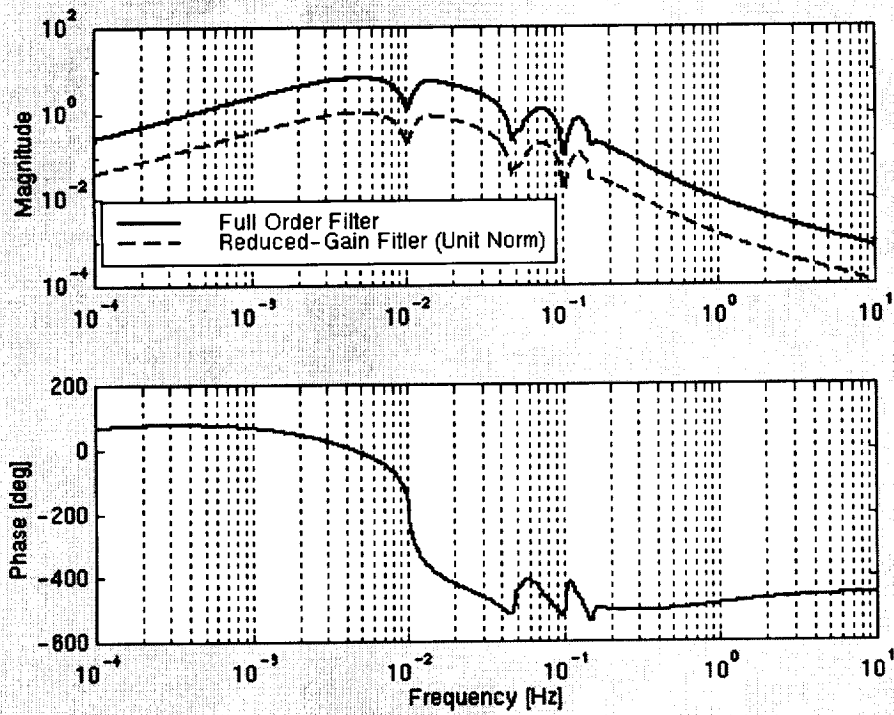


Figure 4. Bode Plot of Bipolar Filter

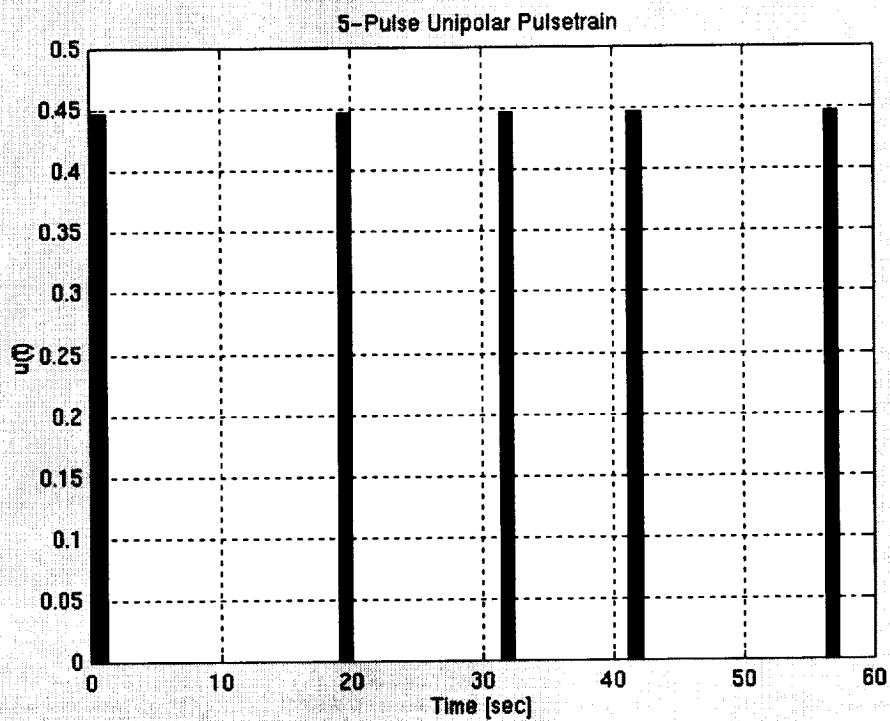


Figure 5. 5-pulse Unipolar Signal

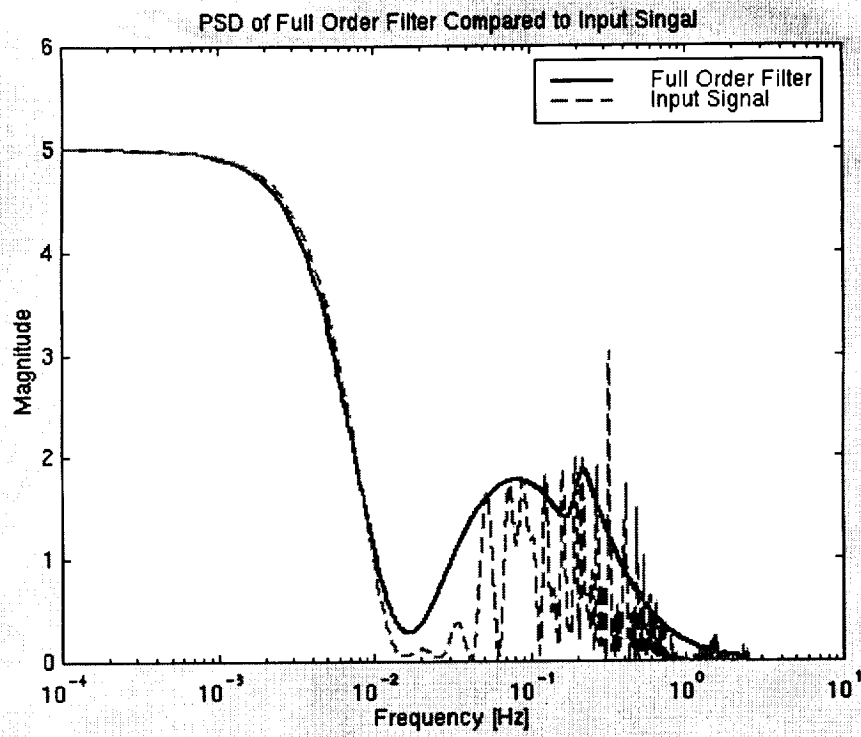


Figure 6. PSD of Filtered Signal Compared to 5-pulse Unipolar Signal

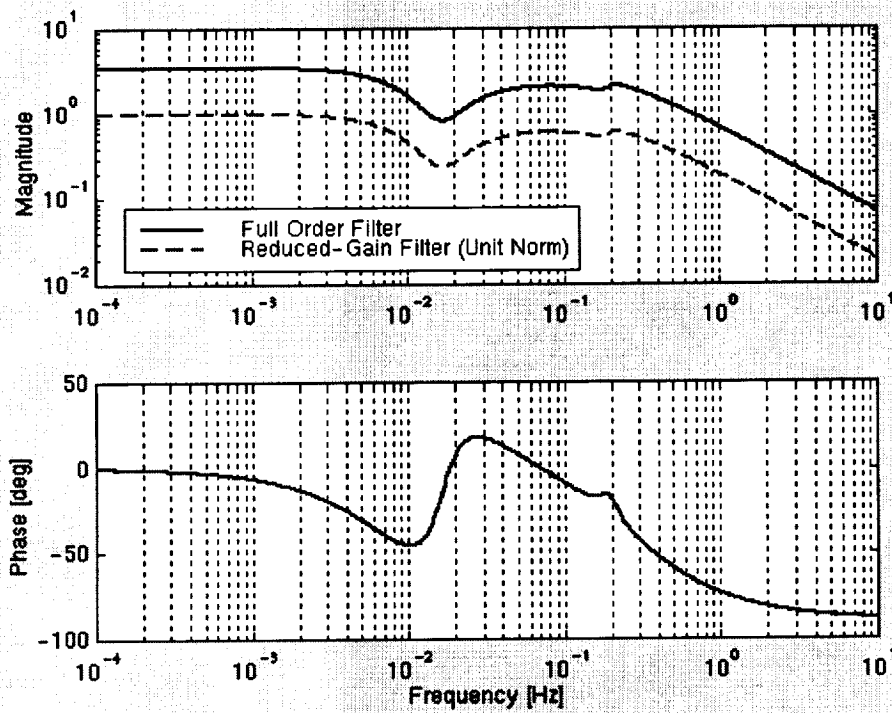


Figure 7. Bode Plot of Unipolar Filter

Table 1. Maximum Joint Torque for ISS 4A US Lab Pitch 180 due to Bipolar Input

| Input | Output | Sim | Unwtd | Wtd | Unwtd/Sim | Wtd/Sim |
|---------|--------|-------|--------|-------|-----------|---------|
| ROLL | SHY | 14.00 | 76.07 | 26.19 | 5.44 | 1.87 |
| | SHP | 22.78 | 97.50 | 41.64 | 4.28 | 1.83 |
| | ELP | 16.69 | 70.05 | 30.20 | 4.20 | 1.81 |
| | WRP | 5.82 | 25.04 | 10.38 | 4.30 | 1.78 |
| | WRY | 3.83 | 26.58 | 8.79 | 6.95 | 2.30 |
| | WRR | 3.15 | 14.47 | 5.43 | 4.60 | 1.73 |
| PITCH | SHY | 42.94 | 241.42 | 62.57 | 5.62 | 1.46 |
| | SHP | 31.41 | 192.81 | 55.98 | 6.14 | 1.78 |
| | ELP | 22.85 | 250.38 | 46.23 | 10.96 | 2.02 |
| | WRP | 16.80 | 186.27 | 34.70 | 11.09 | 2.07 |
| | WRY | 16.43 | 107.28 | 23.84 | 6.53 | 1.45 |
| | WRR | 12.08 | 146.65 | 23.47 | 12.14 | 1.94 |
| YAW | SHY | 31.68 | 240.92 | 63.02 | 7.60 | 1.99 |
| | SHP | 23.23 | 132.24 | 38.19 | 5.69 | 1.64 |
| | ELP | 15.65 | 89.68 | 29.30 | 5.73 | 1.87 |
| | WRP | 6.63 | 57.00 | 11.34 | 8.59 | 1.71 |
| | WRY | 10.31 | 111.87 | 18.12 | 10.85 | 1.76 |
| | WRR | 3.22 | 40.38 | 4.96 | 12.54 | 1.54 |
| ALL | SHY | 27.56 | 349.45 | 92.59 | 12.68 | 3.36 |
| | SHP | 77.35 | 253.31 | 79.53 | 3.28 | 1.03 |
| | ELP | 50.12 | 275.03 | 62.51 | 5.49 | 1.25 |
| | WRP | 23.20 | 196.40 | 37.95 | 8.47 | 1.64 |
| | WRY | 17.83 | 157.26 | 31.21 | 8.82 | 1.75 |
| | WRR | 15.46 | 152.79 | 24.59 | 9.88 | 1.59 |
| Average | | | | | 7.58 | 1.80 |

Table 2. Maximum Joint Torque for ISS 4A due to Unipolar Input Signal.

| Input | Output | Sim | Unwtd | Wtd | Unwtd/Sim | Wtd/Sim |
|---------|--------|-------|--------|----------|-----------|---------|
| ROLL | SHY | 5.51 | 76.07 | 3.61E+01 | 13.81 | 6.55 |
| | SHP | 6.36 | 97.50 | 4.27E+01 | 15.32 | 6.71 |
| | ELP | 3.48 | 70.05 | 3.06E+01 | 20.14 | 8.81 |
| | WRP | 2.03 | 25.04 | 1.13E+01 | 12.35 | 5.55 |
| | WRY | 2.87 | 26.58 | 1.26E+01 | 9.27 | 4.41 |
| | WRR | 2.45 | 14.47 | 6.87E+00 | 5.91 | 2.81 |
| PITCH | SHY | 33.00 | 241.42 | 1.32E+02 | 7.32 | 4.01 |
| | SHP | 22.16 | 192.81 | 1.04E+02 | 8.70 | 4.68 |
| | ELP | 29.30 | 250.38 | 1.32E+02 | 8.55 | 4.51 |
| | WRP | 22.44 | 186.27 | 1.09E+02 | 8.30 | 4.87 |
| | WRY | 15.46 | 107.28 | 6.13E+01 | 6.94 | 3.96 |
| | WRR | 24.26 | 146.65 | 8.55E+01 | 6.04 | 3.52 |
| YAW | SHY | 30.67 | 240.92 | 1.20E+02 | 7.85 | 3.92 |
| | SHP | 18.70 | 132.24 | 6.50E+01 | 7.07 | 3.47 |
| | ELP | 11.43 | 89.68 | 4.32E+01 | 7.85 | 3.78 |
| | WRP | 8.96 | 57.00 | 2.94E+01 | 6.36 | 3.28 |
| | WRY | 16.99 | 111.87 | 5.81E+01 | 6.58 | 3.42 |
| | WRR | 6.85 | 40.38 | 2.13E+01 | 5.89 | 3.10 |
| ALL | SHY | 43.67 | 349.45 | 1.82E+02 | 8.00 | 4.18 |
| | SHP | 34.31 | 253.31 | 1.30E+02 | 7.38 | 3.77 |
| | ELP | 33.32 | 275.03 | 1.42E+02 | 8.26 | 4.28 |
| | WRP | 25.95 | 196.40 | 1.14E+02 | 7.57 | 4.38 |
| | WRY | 29.04 | 157.26 | 8.54E+01 | 5.42 | 2.94 |
| | WRR | 30.73 | 152.79 | 8.84E+01 | 4.97 | 2.87 |
| Average | | | | | 8.58 | 4.32 |